Pergamon

Chemical Engineering Science, Vol. 50, No. 18, pp. 2943–2956, 1995

0009-2509/95 $9.50 + 0.00

0009-2509(95)00126-3

ON THE SLOW MOTION OF AN INTERFACIAL VISCOUS DROPLET IN A THIN LIQUID LAYER

K. D. DANOV
Laboratory of Thermodynamics and Physico-Chemical Hydrodynamics, Faculty of Chemistry, University of Sofia, J. Bourchier Ave. 1, Sofia 1126, Bulgaria

and

R. AUST†, F. DURST and U. LANGE
Lehrstuhl für Strömungsmechanik, Universität Erlangen-Nürnberg, Cauerstr. 4, D-91058 Erlangen, Germany

(*Received* 26 *October* 1994; *accepted in revised form* 6 *March* 1995)

Abstract—In order to investigate the influence of the surface viscosity on the type of the flow inside and outside a droplet moving in a thin liquid layer, it is essential to compute all hydrodynamical parameters which are important for a better understanding of the hydrodynamical interaction of the thin liquid film and the droplet in it. In the present paper, the problem of a translational slow motion of a droplet with a viscous interface in a liquid layer bounded by viscous liquid–gas interfaces is considered. For low Reynolds and capillary numbers, different values of droplet and film bulk viscosity ratios and surface dilatational and shear viscosities are used in the frame of Newtonian surface rheology. The problem reduces to two dimensions when using the "two vorticities–one velocity" formulation of basic flow equations. The model equations and boundary conditions, which contain second-order derivatives of the velocity and the vorticity, are solved numerically to provide information on type of flow, pressure distribution and drag coefficient. The numerical results reveal the strong influence of the surface viscosity on the motion of the droplet in the viscous liquid layer when the radius of the droplet is of the same order of magnitude as the thickness of the liquid film. The presence of the viscous liquid–gas interface close to the droplet changes the flow pattern inside the droplet considerably when the droplet bulk viscosity is sufficiently higher than the viscosity of the film.

1. INTRODUCTION

Coating processes, such as those encountered in the photographic industry, may be significantly influenced by interfacial rheological properties. Coating fluids generally contain molecular species which readily adsorb to the surface of a fluid layer [cf. Valentini *et al.* (1991)]. When the coating film contains liquid or gaseous defects (droplets or bubbles) the species adsorb also to the liquid–liquid or liquid–gas interfaces and they change the rheological behaviour of the interfaces from a free interface to a linear Newtonian or non-Newtonian highly viscous layer. The behaviour is similar to particle interfaces in biological fluid flow systems containing deformable particles. The material properties of the red blood cell membrane and its physiological functions [cf. Feng (1993)] depend on the interfacial viscosity and diffusivity. That is why the theoretical and experimental investigation of the hydrodynamical parameters of the flow induced by the movement of a solid or liquid particle in liquid layers or pipes is one of the important tasks of chemical engineering.

Classical experiments carried out by Lebedev (1916) and Silvey (1916) show that small fluid droplets settled as solid spheres and therefore contradict the theory of Rybczynski (1911) and Hadamard (1911). The small amount of surfactants changes the interfacial mobility of the droplet. The effect of Gibbs elasticity and surface viscosity on the drag coefficient of an emulsion droplet in an adsorption controlled unbounded Marangoni flow was presented by Levich (1962) and Edwards *et al.* (1991). They showed that in the frame of the Boussinesq–Scriven constitutive law for a Newtonian viscous liquid interface, only the dilatational surface viscosity influences the drag. The numerical results of Danov *et al.* (1994) revealed that there is a strong influence of the shear and dilatational surface viscosity on the motion (rotation, translation and stationary) of a solid particle in a viscous liquid layer when the radius of the particle is of the same order of magnitude as the thickness of the liquid film or when the particle is close to the surface of the liquid film.

The hydrodynamics treatment of solid particles, droplets and bubbles in the presence of walls was developed by several authors [cf. Happel and Brenner (1965), Hetsroni (1982) and Davis (1993)]. Here we

†Corresponding author.

point out only some new articles related very close to the topic of the present paper. Shapira and Haber (1988,1990), using Lorentz's reflection method, provided analytical results for the drag force and the shape of a small droplet moving in Couette flow or with constant translational velocity between two parallel walls. Yang and Leal (1990) considered the movement of a spherical droplet, either parallel or perpendicular to a plane, deformable interface in the frame of low Reynolds number hydrodynamics. They investigated the influence of the viscosity ratios, density differences, interfacial tensions and the drop position relative to the free interface on the degree of distortion of the plane interface as well as on the distortion of the fluid drop surface. Besides, they calculated the drag coefficient of the moving droplet.

These analytical results of particle motions close to interfaces are not applicable in the case of a viscous interface because the boundary conditions contain second-order derivatives of the velocity [cf. Danov *et al.* (1994)].

These boundary conditions are the reason, why the otherwise convenient numerical method for solving the problem of a moving rigid particle in Stokes' flow, the second-kind boundary-integral equation formulation as used by Liron and Barta (1992) is not applicable in our case. Similarly, the explicit transient algorithm for predicting incompressible viscous flow in arbitrary geometry given by Mukhopadhyay *et al.* (1993) is valid only with standard boundary conditions. Therefore, we used the "two vorticities–one velocity" formulation, in order to reduce the problem of the moving particle in a thin liquid layer from three dimensions to two dimensions.

The present paper discusses the problem for determining the hydrodynamical parameters of a small droplet moving in a viscous liquid layer for low Reynolds and capillary numbers. At all interfaces a linear Newtonian rheological behaviour is assumed. The problem for Stokes' flow in a cylindrical coordinate system of revolution in the liquid layer and in a spherical coordinate system inside the droplet is reduced from three dimensions to two dimensions using a method similar to that of Danov *et al.* (1994). It turned out that the application of this method is convenient for numerical computations. In order to illustrate the global interaction between a droplet and an interface and its dependence on the bulk viscosity ratios, the surface viscosity numbers and the drag force, velocity and pressure distributions outside as well as inside the droplet were obtained and are presented in Section 3. The numerical results reveal the change of the type of motion inside the droplet when the droplet bulk viscosity is sufficiently higher than the film bulk viscosity. The effects depend strongly on the magnitude of the surface viscosity.

2. MATHEMATICAL MODEL OF THE PROBLEM. BASIC EQUATIONS AND BOUNDARY CONDITIONS

Let us consider a viscous liquid droplet with radius a and viscous interface S_d performing a translational motion along the Oy axis. The droplet is immersed in a viscous liquid layer bounded by two viscous interfaces S_1 and S_2 (see Fig. 1). It is supposed that the translational velocity V_* of the droplet is so slow and the deformation of the interfaces S_1, S_2 and S_d caused by the flow are so small that the flow inside the droplet as well as the flow in the surrounding liquid film can be considered as a viscous, incompressible creeping motion and that all the boundary conditions can be linearized around the non-perturbed interfaces. As was shown in Danov *et al.* (1994) the solution of Stokes' equations in the liquid layer contains only one mode of the Fourier expansion. After introducing dimensionless variables by scaling the r-, z- and x_1-coordinates with the droplet radius a (see Fig. 1) the components of the velocity in the liquid film $\mathbf{v}^f$ and the pressure p^f can be expressed in the following general form:

$$v_r^f = V_*\left[\frac{\partial}{\partial r}(rF^f) - \psi\right]\sin\varphi, \quad v_\varphi^f = V_* F^f \cos\varphi$$
$$v_z^f = V_*\left[\frac{\partial}{\partial z}(rF^f) - \zeta\right]\sin\varphi, \quad p^f = \frac{\eta^f V_*}{a} P^f \sin\varphi \tag{1}$$

where ψ and ζ are dimensionless functions related to the vorticity components in the meridian plane, F^f and P^f are the dimensionless meridian components of the velocity and pressure and η^f is the viscosity of the liquid. Let the non-perturbed equations of the film interfaces are $z = z_1$ and $z = z_2$, where z_1 and z_2 are the vertical coordinates of the liquid layer planes. Following the method for the transformation of the three-dimensional problem into a two-dimensional problem using the "two vorticities–one velocity" for mulation, the Fourier expansion of the components of the velocity $\mathbf{v}^d$ and the pressure p^d inside the droplet can be written as follows:

$$v_1^d = V_* \sin x_2\left[\frac{\partial}{\partial x_1}(F^d x_1) + 2w_2^d x_1\right]\sin\varphi,$$
$$v_\varphi^d = V_* F^d \cos\varphi$$
$$v_2^d = V_*\left[\frac{\partial}{\partial x_2}(F^d \sin x_2) - 2w_1^d x_1 \sin x_2\right]\sin\varphi, \tag{2}$$
$$p^d = \frac{\eta^d V_*}{a} P^d \sin\varphi$$

where F^d, P^d, w_1^d and w_2^d are the dimensionless meridian components of the fluid velocity, pressure, and

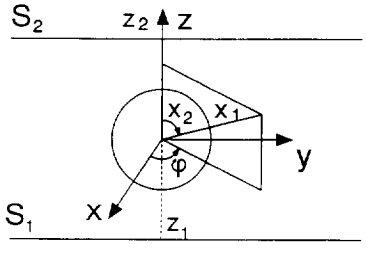

Fig. 1. Geometry of the system.

radial and polar components of the vorticity vector, respectively, and η^d is the viscosity of the liquid inside the droplet.

Substituting eqs (1) and (2) into the equations of continuity [cf. Danov *et al.* (1994)] we obtain the following equations for F^f and F^d in the liquid layer and inside the droplet:

$$\frac{\partial^2 F^f}{\partial r^2}+\frac{3}{r}\frac{\partial F^f}{\partial r}+\frac{\partial^2 F^f}{\partial z^2}-\frac{1}{r}\frac{\partial \psi}{\partial r}-\frac{\psi}{r^2}-\frac{1}{r}\frac{\partial \zeta}{\partial z}=0$$

$$\frac{\partial^2 F^d}{\partial x_1^2}+\frac{4}{x_1}\frac{\partial F^d}{\partial x_1}+\frac{1}{x_1^2}\frac{\partial^2 F^d}{\partial x_2^2}+\frac{3\cot x_2}{x_1^2}\frac{\partial F^d}{\partial x_2}+2\left(\frac{\partial w_2^d}{\partial x_1}+\frac{3w_2^d}{x_1}\right)-\frac{2}{x_1}\left(\frac{\partial w_1^d}{\partial x_2}+2w_1^d\cot x_2\right)=0. \tag{3}$$

After eliminating the pressure from Stokes' equations one obtains a general equation for the vorticity vector. This yields the following system of second-order differential equations for the vorticity functions ψ and ζ in the liquid layer:

$$\frac{\partial^2 \psi}{\partial r^2}-\frac{1}{r}\frac{\partial \psi}{\partial r}+\frac{\partial^2 \psi}{\partial z^2}=0$$

$$\frac{\partial^2 \zeta}{\partial r^2}+\frac{1}{r}\frac{\partial \zeta}{\partial r}+\frac{\partial^2 \zeta}{\partial z^2}-\frac{\zeta}{r^2}-\frac{2}{r}\frac{\partial \psi}{\partial z}=0. \tag{4}$$

Using an analogous procedure for the dimensionless radial and polar coordinates of the vorticity vector inside the droplet, we obtain a similar system in spherical coordinates:

$$\frac{\partial^2 w_1^d}{\partial x_1^2}+\frac{4}{x_1}\frac{\partial w_1^d}{\partial x_1}+\frac{1}{x_1^2}\frac{\partial^2 w_1^d}{\partial x_2^2}+\frac{\cot x_2}{x_1^2}\frac{\partial w_1^d}{\partial x_2}+\frac{w_1^d}{x_1^2}(1-\cot^2 x_2)=0$$

$$\frac{\partial^2 w_2^d}{\partial x_1^2}+\frac{2}{x_1}\frac{\partial w_2^d}{\partial x_1}+\frac{1}{x_1^2}\frac{\partial^2 w_2^d}{\partial x_2^2}+\frac{3\cot x_2}{x_1^2}\frac{\partial w_2^d}{\partial x_2}-\frac{2w_2^d}{x_1^2}+\frac{2\cot x_2}{x_1}\frac{\partial w_1^d}{\partial x_1}+\frac{2}{x_1^2}\frac{\partial w_1^d}{\partial x_2}+\frac{4\cot x_2}{x_1^2}w_1^d=0. \tag{5}$$

Once the solution (F^f, ψ, ζ, F^d, w_1^d and w_2^d) of the eqs (2)–(5) is found, the velocity components outside as well as inside the droplet can be computed using eqs (1) and (2). By substituting eqs (1) and (2) into the meridian components of the momentum balance, the pressures inside and outside can be expressed in terms of the solution of eqs (3)–(5) as follows:

$$P^f=\frac{\partial \psi}{\partial r}-\frac{\psi}{r}+\frac{\partial \zeta}{\partial z},$$

$$P^d=2\sin x_2\left(\frac{\partial w_1^d}{\partial x_2}-x_1\frac{\partial w_2^d}{\partial x_1}-w_2^d\right). \tag{6}$$

In order to account for the influence of soluble and insoluble surfactants, when the Marangoni effect is neglected and the interface rheology is linear, we consider the Boussinesq–Scriven definition for the Newtonian interfaces [cf. Scriven (1960) and Edwards *et al.* (1991)]. In this case, the surface excess pressure tensor can be written as a sum of the isotropic thermodynamic interfacial tensor and deviatoric parts, which are related to the surface excess stress tensor. The surface excess stress tensor in the frame of the linear interfacial rheology depends on the rate of relative displacement of surface points and the dilatational and shear viscosities, which are the material properties of the fluid interface. In the dimensionless formulation the Boussinesq–Scriven definition yields the following parameters:

$$\mu^f=\frac{\eta^f}{\eta_*},\ \mu^d=\frac{\eta^d}{\eta_*},\ K_d=\frac{\eta_d^d}{\eta_*},\ E_d=\frac{\eta_{\mathrm{sh}}^d}{\eta_*}$$

$$E_k=\frac{\eta_{\mathrm{sh},k}}{a\eta_*},\ K_k=\frac{\eta_{d,k}}{a\eta_*}\quad (k=1,2) \tag{7}$$

where μ^f and μ^d are the ratios of the bulk viscosities and the characteristical viscosity η_*. E_k and E_d are shear surface viscosity numbers, K_k and K_d are dilatational surface viscosity numbers of liquid–gas and liquid–liquid interfaces, $\eta_{\mathrm{sh},k}$, $\eta_{d,k}$, η_{sh}^d and η_d^d are, respectively, the interfacial shear and dilatational viscosities at a given point of the liquid–gas and the droplet interface. Hence, in the "two vorticities–one velocity" formulation the kinematical equation and the tangential projection for the interfacial momentum transport equation on the liquid–gas interfaces give the following boundary conditions [cf. Danov *et al.* (1994)]

$$(-1)^k\mu^f\frac{\partial F^f}{\partial z}=(K_k+E_k)\left(\frac{\partial^2 F^f}{\partial r^2}+\frac{3}{r}\frac{\partial F^f}{\partial r}\right)-\frac{K_k}{r}\frac{\partial \psi}{\partial r}-(K_k+2E_k)\frac{\psi}{r^2}$$

$$(-1)^k\mu^f\frac{\partial \psi}{\partial z}=E_k\left(\frac{\partial^2 \psi}{\partial r^2}-\frac{1}{r}\frac{\partial \psi}{\partial r}\right)$$

$$\frac{\partial}{\partial z}(rF^f)=\zeta\quad \text{at } S_k\ (k=1,2). \tag{8}$$

On the droplet surface the fluid velocity inside and outside contains only a component tangential to the surface and it is equal to the mass-average (material) surface velocity. In our case these boundary conditions reduce to

$$\frac{\partial F^d}{\partial x_1}+F^d=-2w_2^d,\quad \frac{\partial F^f}{\partial x_1}+F^f=-2w_2^f$$

$$F^d=F^f=U_\varphi,\ w_1^d=w_1^f=w_1\quad \text{at } S_d \tag{9}$$

where U_φ is the dimensionless meridian component of the interface velocity and w_1 is the dimensionless radial component of the vorticity on the interface (it can be introduced because the radial component of the vorticity is a continuous function on the interface). We consider a similar rheological behaviour of the liquid–liquid droplet interface S_d as of the liquid–gas

interfaces S_1 and S_2. Then the dynamic boundary conditions in the "two vorticities-one velocity" formulation reduce to

$$\frac{\partial}{\partial x_1}(\mu^d F^d - \mu^f F^f) - (\mu^d - \mu^f)U_\varphi = (K_d + E_d)\left(\frac{\partial^2 U_\varphi}{\partial x_2^2} + 3\cot x_2 \frac{\partial U_\varphi}{\partial x_2}\right) - 2K_d U_\varphi - 2K_d \frac{\partial w_1}{\partial x_2} - 4(K_d + E_d)\cot x_2 w_1 \tag{10}$$

$$\frac{\partial}{\partial x_1}(\mu^d w_1^d - \mu^f w_1^f) = E_d\left[\frac{\partial^2 w_1}{\partial x_2^2} + \cot x_2 \frac{\partial w_1}{\partial x_2} + (1 - \cot^2 x_2) w_1\right].$$

In the surface equations and boundary conditions (7)–(9) the spherical vorticity components in the liquid layer are related to the functions ψ and ζ as follows:

$$w_1^f = -\frac{1}{2x_1}(\psi + \zeta\cot x_2), \quad w_2^f = \frac{1}{2x_1}(\psi\cot x_2 - \zeta). \tag{11}$$

Finally, the resultant force **F**, due to the stresses, exerted by the surrounding fluid on the surface of the droplet S_d can be derived from

$$F_x = 0, \quad F_y = f\pi a\eta_* V_*, \quad F_z = 0 \tag{12}$$

where the dimensionless drag coefficient f is

$$f = \int_0^\pi \left(-P^f + \frac{\partial R^f}{\partial r} + \frac{\partial F^f}{\partial r} - \frac{\partial Z^f}{\partial z}\right)\sin^2 x_2 \, dx_2 + \int_0^\pi \left(\sin x_2 \frac{\partial R^f}{\partial z} + \sin x_2 \frac{\partial Z^f}{\partial r} + \sin x_2 \frac{\partial F^f}{\partial z} + Z^f\right)\cos x_2 \, dx_2 \tag{13}$$

and the dimensionless radial and vertical film velocity components R^f and Z^f are given by

$$R^f = \frac{\partial}{\partial r}(rF^f) - \psi, \quad Z^f = \frac{\partial}{\partial z}(rF^f) - \zeta \tag{14}$$

Integration of eq. (13) is performed along the non-perturbed droplet boundary $x_1 = 1$.

3. NUMERICAL RESULTS AND DISCUSSIONS

3.1. *Velocity and pressure distribution*

In Figs 2–7, velocity and pressure distributions for a droplet moving in a thin liquid layer are presented. As opposed to the case, when a droplet is moving in an unbounded liquid, one observes immediately, that the velocity fields as well as the pressure distributions are no longer symmetrical. This is due to the presence of the interfaces close to the droplet with different distances from the lower and upper side. Besides, the lower surface viscosity numbers were chosen to be ten times higher than the upper ones.

The fact that the droplet is closer to the lower interface means that there is less liquid to be moved by the particle between its surface and the interface than on the upper side and, hence, this will reduce the size of the vortex inside the droplet on the lower side. In contrast, the higher viscosity of the lower interface tends to increase the size of the corresponding lower vortex.

In Fig. 2 the effect of the different distances to the lower and upper interface and the effect of the different surface viscosity numbers neutralise each other approximately so that the two vorticities have about the same size. In Fig. 2(a) the viscosity inside the droplet is ten times lower than in the situation which was considered for Fig. 2(b). One observes that the flow pattern does not change but that the absolute values of the velocity inside the droplet decrease due to the increased dissipation of energy.

In contrast, changing only the viscosity of the film, whilst all other parameters remain constant, changes the flow pattern inside and outside the droplet dramatically, as can be seen from Fig. 3. One can see that for a higher film viscosity the influence of the particle is further reaching and the gradients are less pronounced, than for smaller film viscosities. When the viscosity of the film and the droplet are of the same order of magnitude, the situation is similar to the previously described case. However, when the droplet viscosity exceeds the film viscosity by one to two orders of magnitude, the droplet behaves almost like a rigid sphere. When the obtained results are compared with the results presented in Danov *et al.* (1994) one has to bear in mind, that the results presented here refer to the equilibrium situation, not to the elementary motion.

Figures 4 and 5 show the pressure distributions which correspond to the previously discussed velocity plots. In general, the influence of different parameters can be identified easier when looking at the isobars than from the velocity fields. As long as the viscosity of the droplet is smaller or about as high as the viscosity of the film, a change of the droplet viscosity does mainly influence the pressure distribution inside, while there are almost no changes in the film.

From Fig. 4 one can see how an increase of the droplet viscosity leads to lower pressure gradients as well as lower absolute values of the pressure and hence a lower pressure jump at the droplet–film interface.

The situation is rather different when the droplet viscosity is considerably higher than the film viscosity. In this case (Fig. 5) the pressure distribution in the film gets strongly influenced when changing the droplet viscosity. When the film is a lot less viscous than the droplet, the pressure inside the droplet is almost zero as can be expected for a rotating particle. At the same time, the pressure gradients and the absolute values of the pressure in the film are considerably higher and the influence of the surface viscosity results in extremely steep pressure gradients between the bottom of the particle and the lower interface.

In Figs 6 and 7, the presented data refer to a situation with almost free surfaces. When the viscosity of

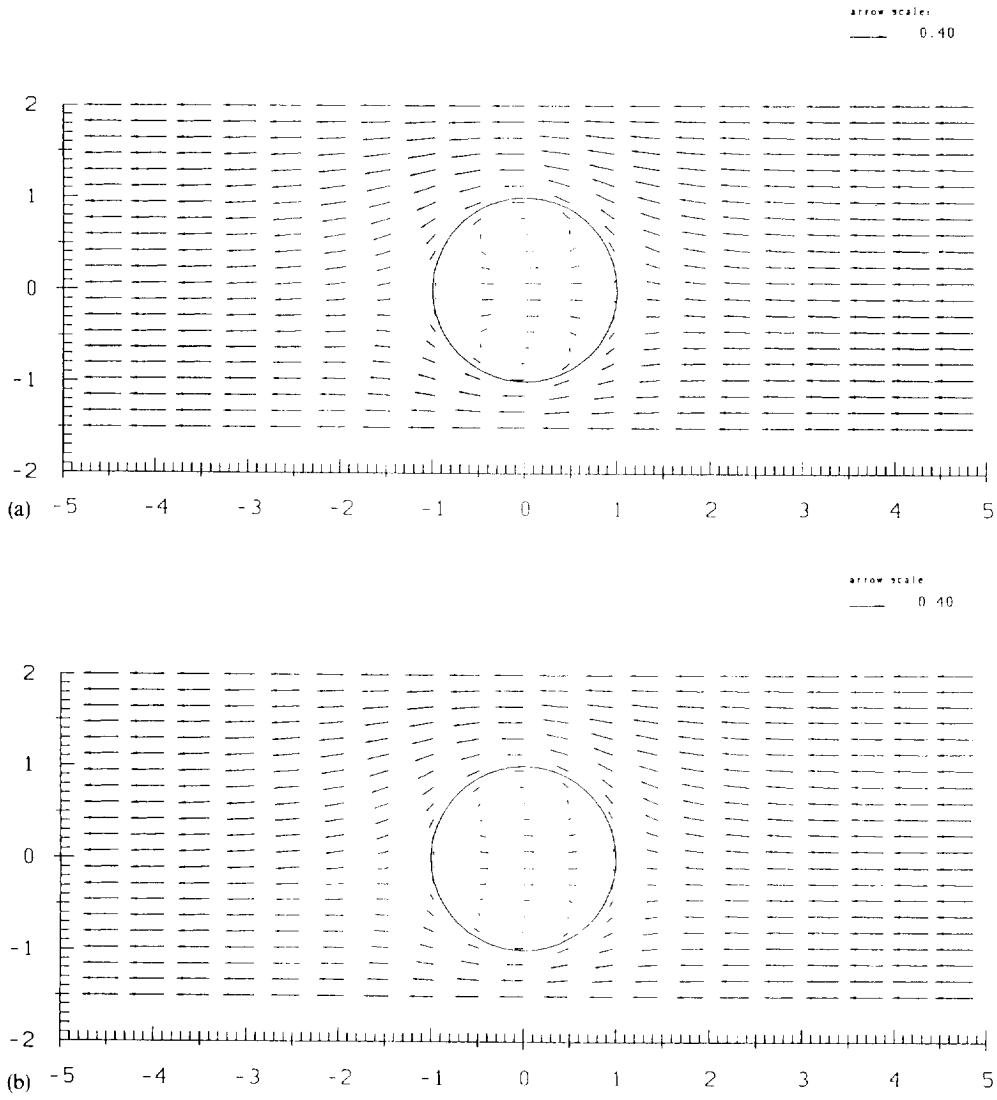

Fig. 2. Velocity field for a droplet moving in the plane $x = 0$ for $z_1 = -1.5$ and $z_2 = 2.0$; $K_d = 1.0$ and $E_d = 1.0$, $K_1 = 1.0$ and $E_1 = 1.0$, $K_2 = 0.1$ and $E_2 = 0.1$, $\mu^f = 1.0$ and two different values of the drop bulk viscosity ratio: (a) $\mu^d = 0.1$ and (b) $= \mu^d = 1.0$.

the droplet is as high as the film viscosity [Fig. 6(a)], one observes that the upper vortex inside the droplet is larger because more liquid is present above the droplet than below. Reducing the film viscosity by 50% does not change the picture qualitatively but the absolute values of the velocity inside the droplet decrease due to the reduced friction. The absolute value of the velocity is in the above cases comparatively small, because energy dissipation at the droplet–film interface is large due to the higher surface viscosity number at this interface.

The corresponding pressure distributions depicted in Fig. 7(a) and (b) show more clearly that changing the film viscosity does not, virtually, alter the flow pattern outside the droplet but significantly influences the flow inside. When comparing Fig. 7(b) with Fig. 5(a), which differ only in the magnitude of the lower surface viscosity number, one notes that the surface properties do have an influence on the whole flow field outside the droplet. For higher value of the surface viscosity, the pressure reaches higher values and especially in the region directly below the droplet one observes high pressure gradients.

3.2. *Influence of the motion inside the droplet on the bulk viscosity ratios*

Figure 8 represents some blow-ups of the situation inside the droplets in order to give the reader a better resolved picture of the different effects. Figure 8(a) and (b) refer to the same situation as in Fig. 2(a) and (b) when the lower surface viscosity number is ten times higher than the upper one and the droplet viscosity gets increased by a factor ten. From these pictures one can see more clearly that the effect of having less liquid below the droplet than above, which would weaken the lower vortex in the droplet and the higher

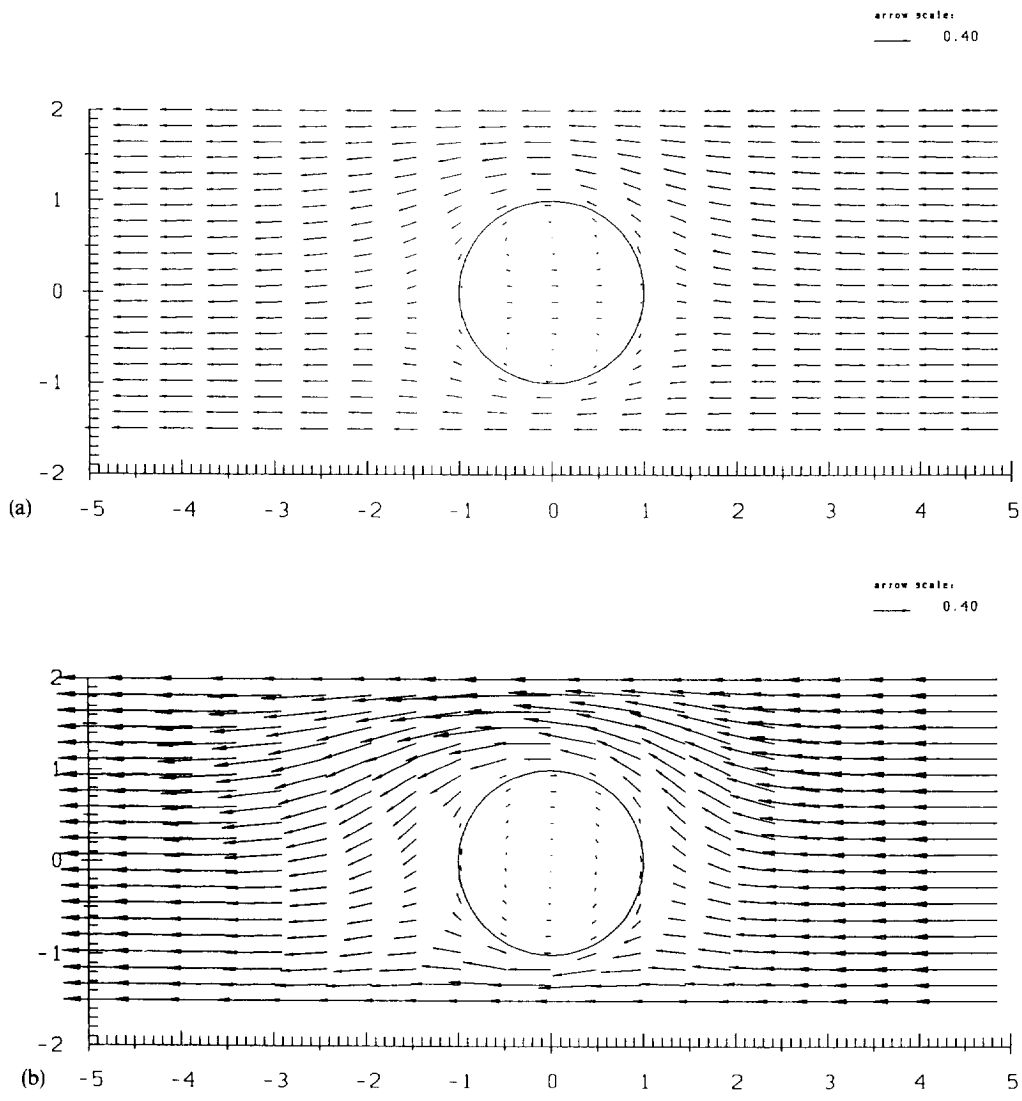

Fig. 3. Velocity field for a droplet moving in the plane $x = 0$ for $z_1 = -1.5$ and $z_2 = 2.0$, $K_d = 1.0$ and $E_d = 1.0$, $K_1 = 1.0$ and $E_1 = 1.0$, $K_2 = 0.1$ and $E_2 = 0.1$, $\mu^d = 1.0$ and two different values of the film bulk viscosity ratio: (a) $\mu^f = 0.5$ and (b) $\mu^f = 0.003$.

friction with the lower interface, which drives this vortex, almost balance each other. Hence, an almost symmetrical flow pattern is resulting. The balance of the two effects is not changed when increasing the droplet viscosity, only the energy dissipation grows and therefore the absolute values of the velocity drop.

From Fig. 8(c)–(e) one can observe that a decrease of the film viscosity relative to the droplet viscosity and the surface viscosity eventually leads to the disappearance of the upper vortex. This is due to the fact that the influence of different amounts of fluid above and below the droplet is less important at low film viscosities whereas the influence of the higher surface viscosity at the lower interface remains the same. However, it has to be noted that such a change in the characteristic of the flow pattern occurs only when the film viscosity is more than one order of magnitude smaller than the droplet and the surface viscosity. We would like to point out that these variations of the viscosity ratios are not of purely academic interest but refer to practically important situations, i.e. Fig. 8(b) is comparable to a droplet of light oil moving in water whereas Fig. 8(e) would represent an emulsion with heavy oil.

3.3. *Shapes of the film and the droplet*

The presence of a droplet in a film with a thickness comparable to the droplet diameter will of course lead to a deformation of the film surface. This deformation is shown for two different cases in Fig. 9, the black arrow indicating the relative velocity between the droplet and the film. When the film viscosity is small compared to the droplet and the surface viscosity, the deformation is a lot larger than in the case when all

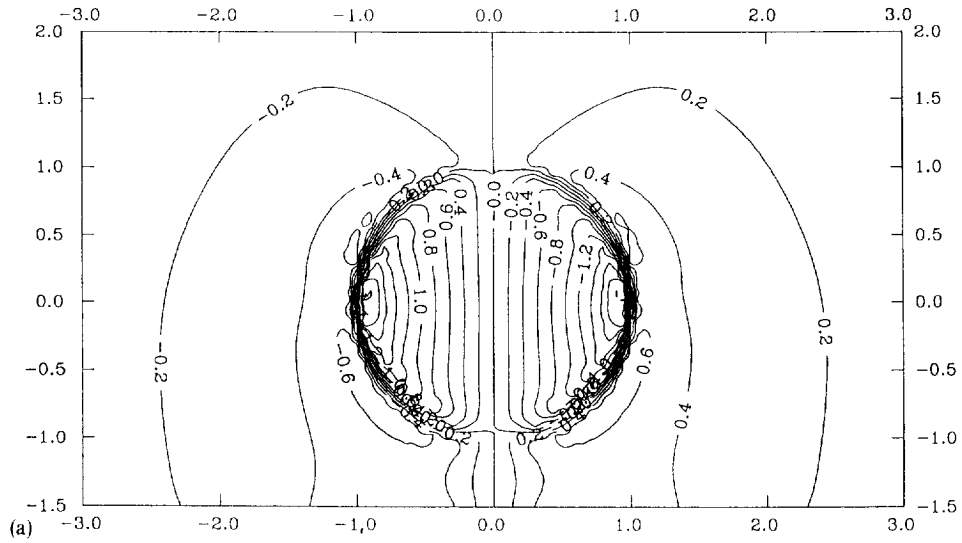

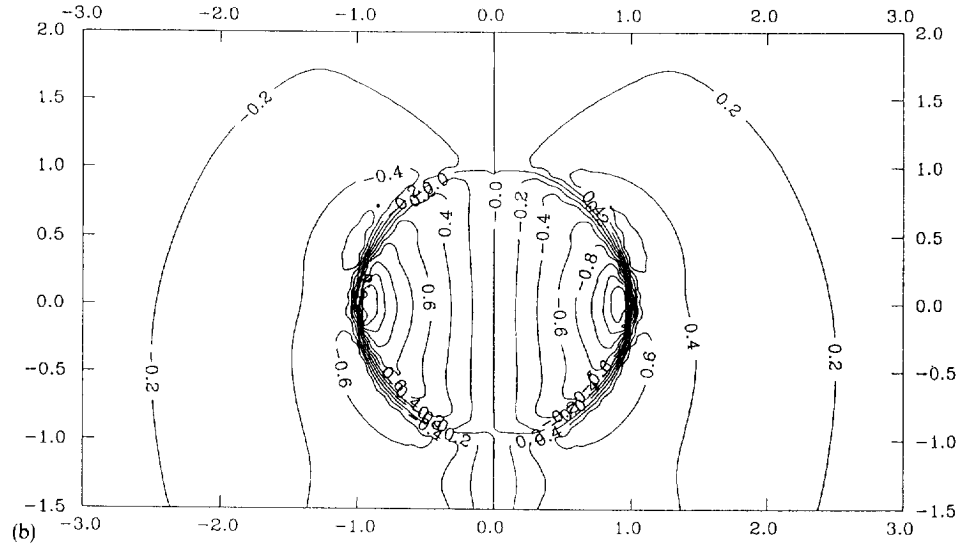

Fig. 4. Pressure distribution for a droplet moving in the plane $x = 0$ for $z_1 = -1.5$ and $z_2 = 2.0$, $K_d = 1.0$ and $E_d = 1.0$, $K_1 = 1.0$ and $E_1 = 1.0$, $K_2 = 0.1$ and $E_2 = 0.1$, $\mu^f = 1.0$ and two different values of the drop bulk viscosity ratio: (a) $\mu^d = 0.1$ and (b) $\mu^d = 1.0$.

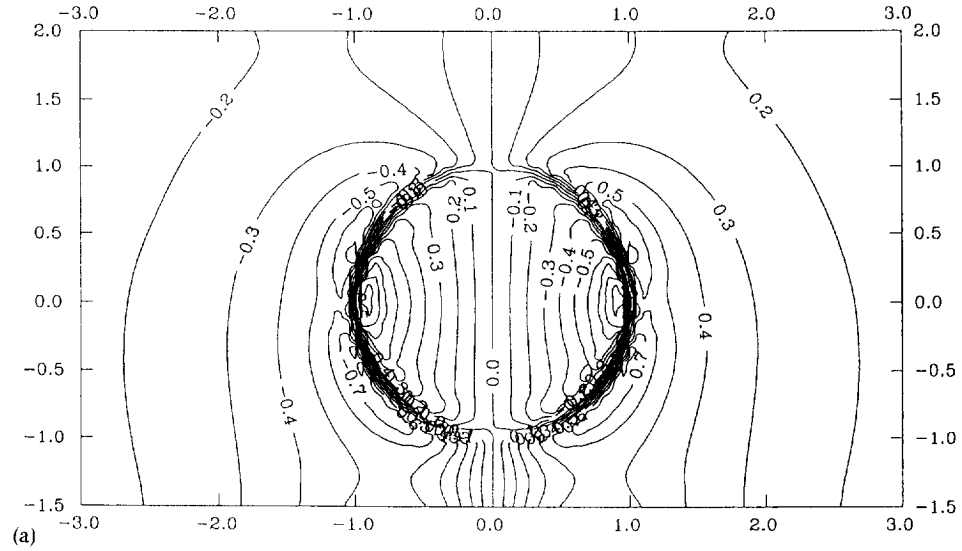

Fig. 5(a).

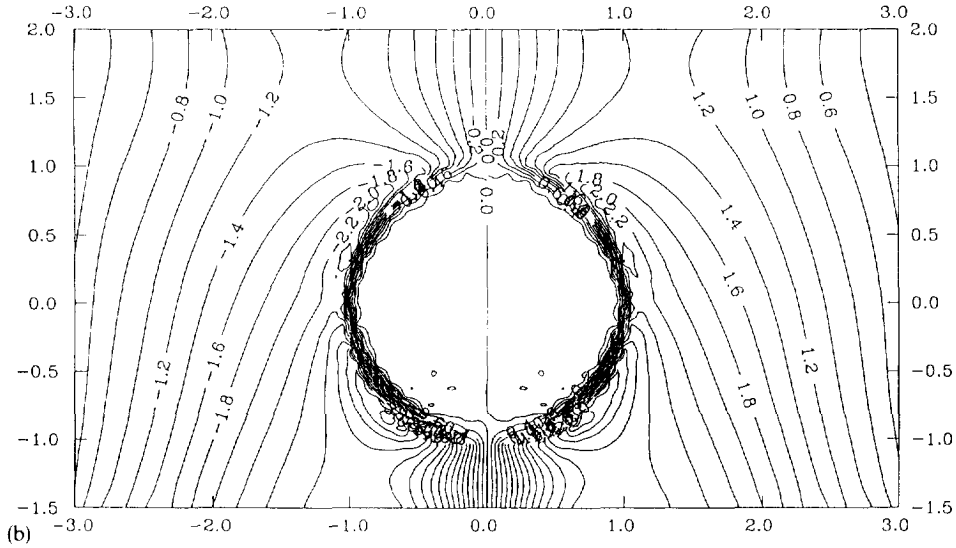

Fig. 5. Pressure distribution for a droplet moving in the plane $x = 0$ for $z_1 = -1.5$ and $z_2 = 2.0$, $K_d = 1.0$ and $E_d = 1.0$, $K_1 = 1.0$ and $E_1 = 1.0$, $K_2 = 0.1$ and $E_2 = 0.1$, $\mu^d = 1.0$ and two different values of the film bulk viscosity ratio: (a) $\mu^f = 0.5$ and (b) $\mu^f = 0.003$.

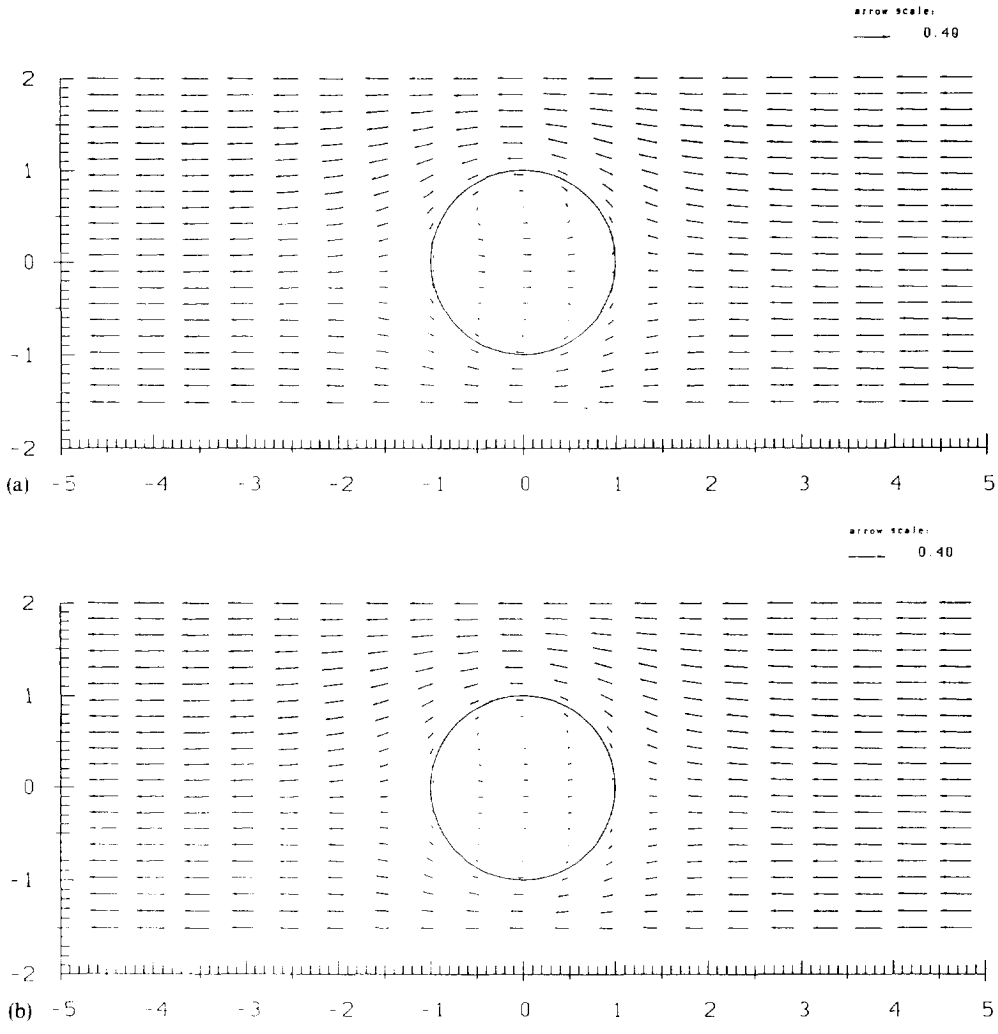

Fig. 6. Velocity field for a droplet moving in the plane $x = 0$ for $z_1 = -1.5$ and $z_2 = 2.0$, $K_d = 1.0$ and $E_d = 1.0$, $K_1 = 0.1$ and $E_1 = 0.1$, $K_2 = 0.1$ and $E_2 = 0.1$, $\mu^d = 1.0$ and two different values of the film bulk viscosity ratio: (a) $\mu^f = 1.0$ and (b) $\mu^f = 0.5$.

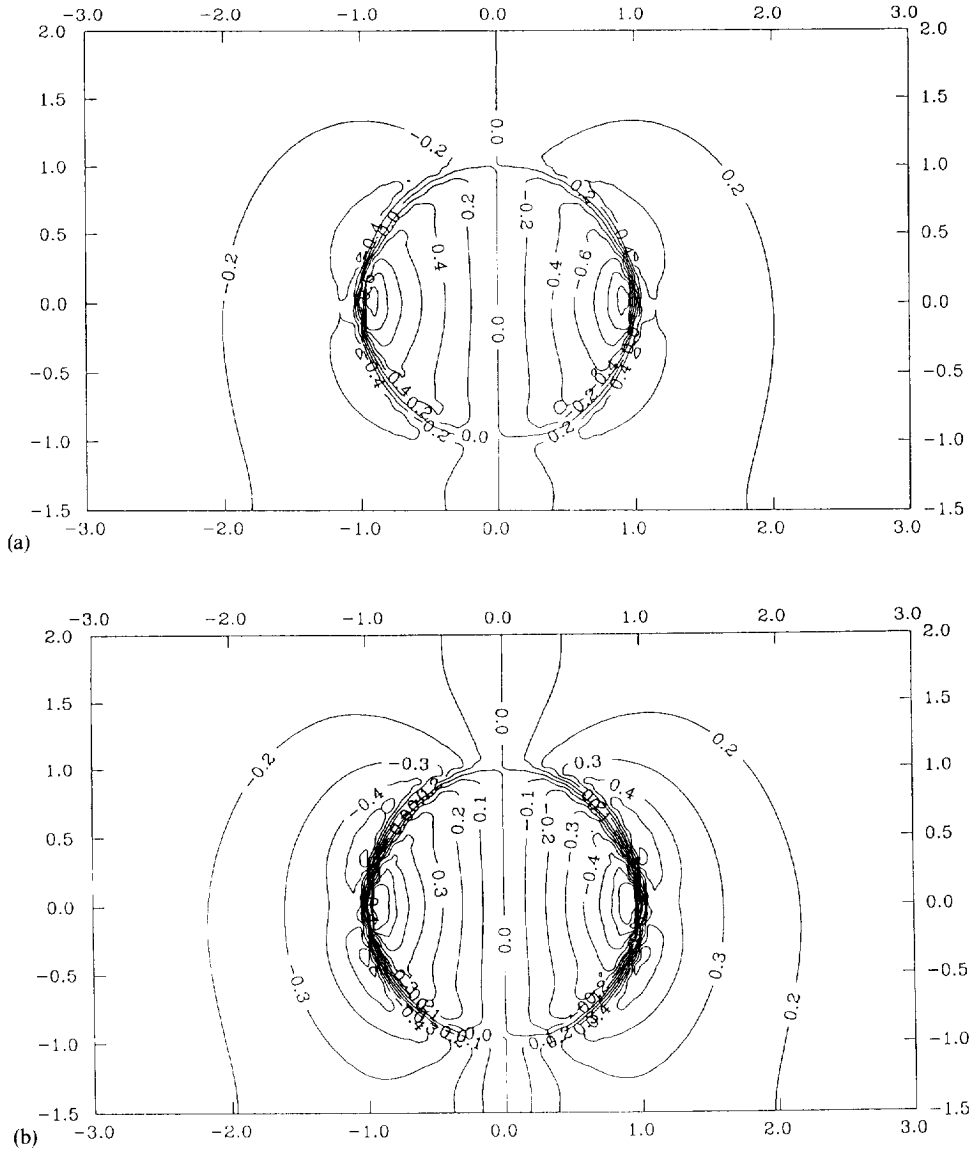

Fig. 7. Pressure distribution for a droplet moving in the plane $x = 0$ for $z_1 = -1.5$ and $z_2 = 2.0$, $K_d = 1.0$ and $E_d = 1.0$, $K_1 = 0.1$ and $E_1 = 0.1$, $K_2 = 0.1$ and $E_2 = 0.1$, $\mu^d = 1.0$ and two different values of the film bulk viscosity ratio: (a) $\mu^f = 1.0$ and (b) $\mu^f = 0.5$.

Table 1. Drag coefficient for $z_1 = -1.5$ and $z_2 = 2.0$, $K_d = 1.0$ and $E_d = 1.0$, $K_2 = 0.1$ and $E_2 = 0.1$ and $\mu^d = 1.0$

μ^f	Shapira and Haber	$K_1 = 1.0$ and $E_1 = 1.0$	$K_1 = 0.1$ and $E_1 = 0.1$
1.0	7.43500	3.12725	2.44373
0.5	8.10382	3.37691	2.66822
0.2	8.79429	3.98537	3.11351
0.003	9.49253	8.55732	8.17554

Table 2. Drag coefficient for $z_1 = -1.5$ and $z_2 = 2.0$, $K_d = 1.0$ and $E_d = 1.0$, $K_2 = 0.1$ and $E_2 = 0.1$ and $\mu^f = 1.0$

μ^d	Shapira and Haber	$K_1 = 1.0$ and $E_1 = 1.0$	$K_1 = 0.1$ and $E_1 = 0.1$
1.0	7.43500	3.12725	2.44373
0.8	7.21687	3.10910	2.43453
0.1	6.21775	3.00772	2.38109

viscosities are of the same order of magnitude. This is easy to understand when looking at the pressure distributions corresponding to Fig. 9(a) (7(a)), and Fig. 9(b) (5(b)).

3.4. *Drag coefficient*

We produced Tables 1 and 2 to allow a comparison between our results and the results of Shapira and Haber (1988, 1990) for a viscous droplet with a free

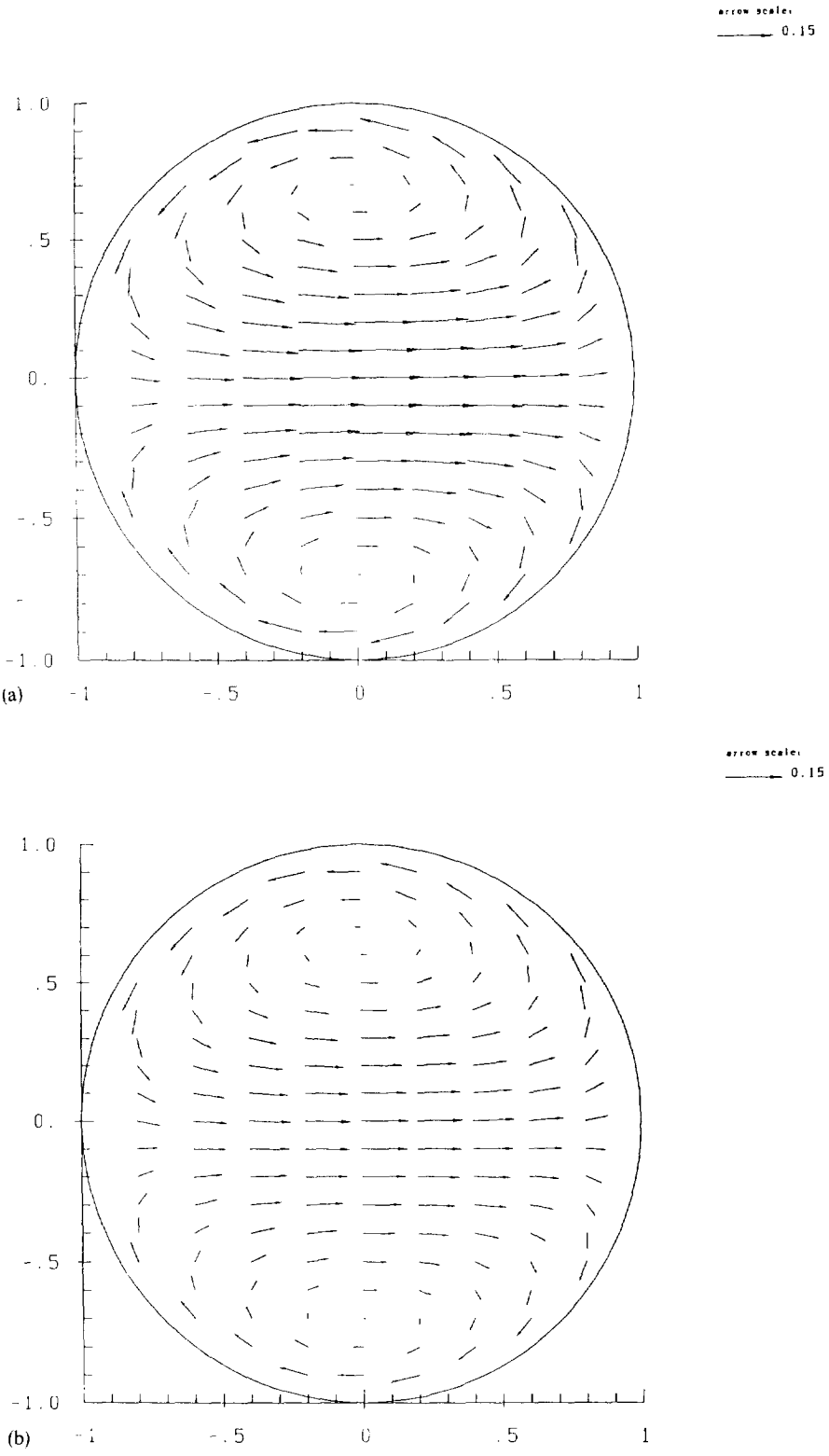

Fig. 8(a) and (b).

surface, moving between two solid walls. In Table 1 we consider the influence of the film viscosity on the drag coefficient for two different values of the lower surface viscosity numbers. When the ratio of film viscosity to droplet viscosity decreases, the drag coefficient increases for all sorts of interfaces. One can see from the calculated values that the drag exerted on the particle for cases where the film viscosity is of the

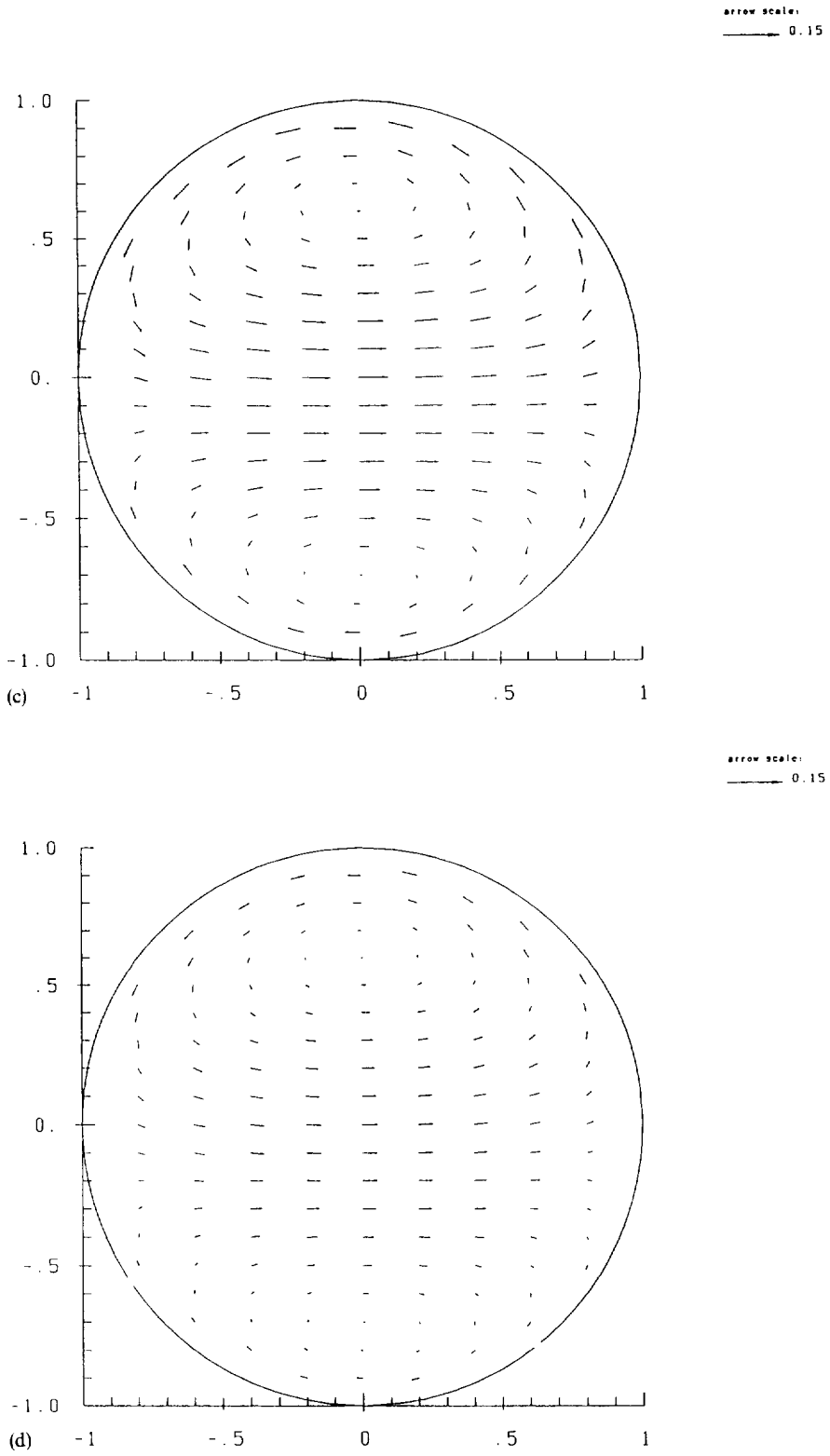

Fig. 8(c) and (d).

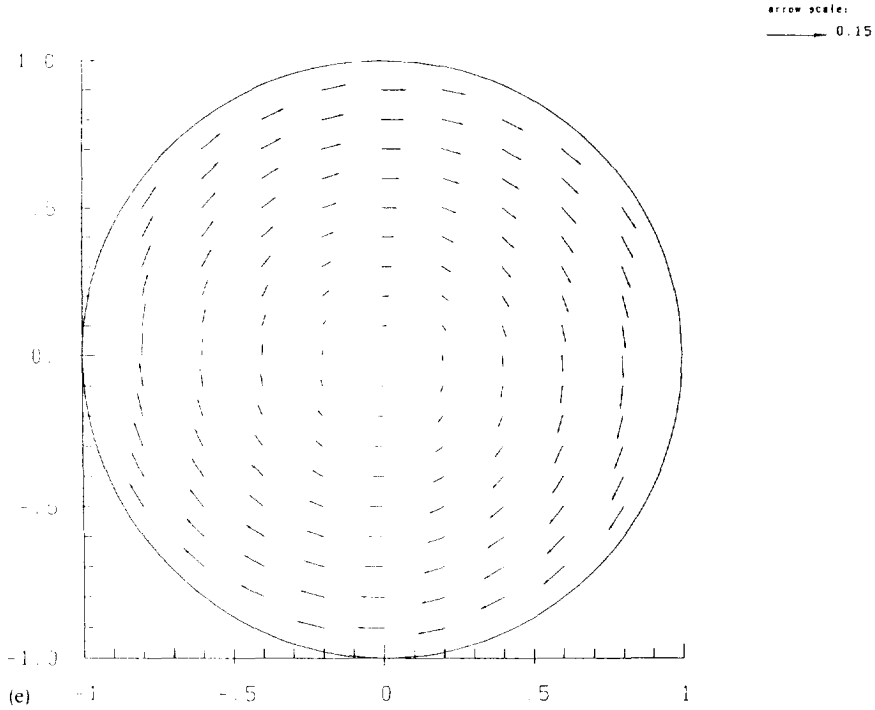

Fig. 8. Change of the vorticity inside the droplet for $z_1 = -1.5$ and $z_2 = 2.0$, $K_d = 1.0$ and $E_d = 1.0$, $K_1 = 1.0$ and $E_1 = 1.0$, $K_2 = 0.1$ and $E_2 = 0.1$ vs the bulk viscosity ratios: (a) $\mu^f = 1.0$, $\mu^d = 0.1$, (b) $\mu^f = 1.0$, $\mu^d = 1.0$, (c) $\mu^f = 0.5$, $\mu^d = 1.0$, (d) $\mu^f = 0.2$, $\mu^d = 1.0$ and (e) $\mu^f = 0.003$, $\mu^d = 1.0$.

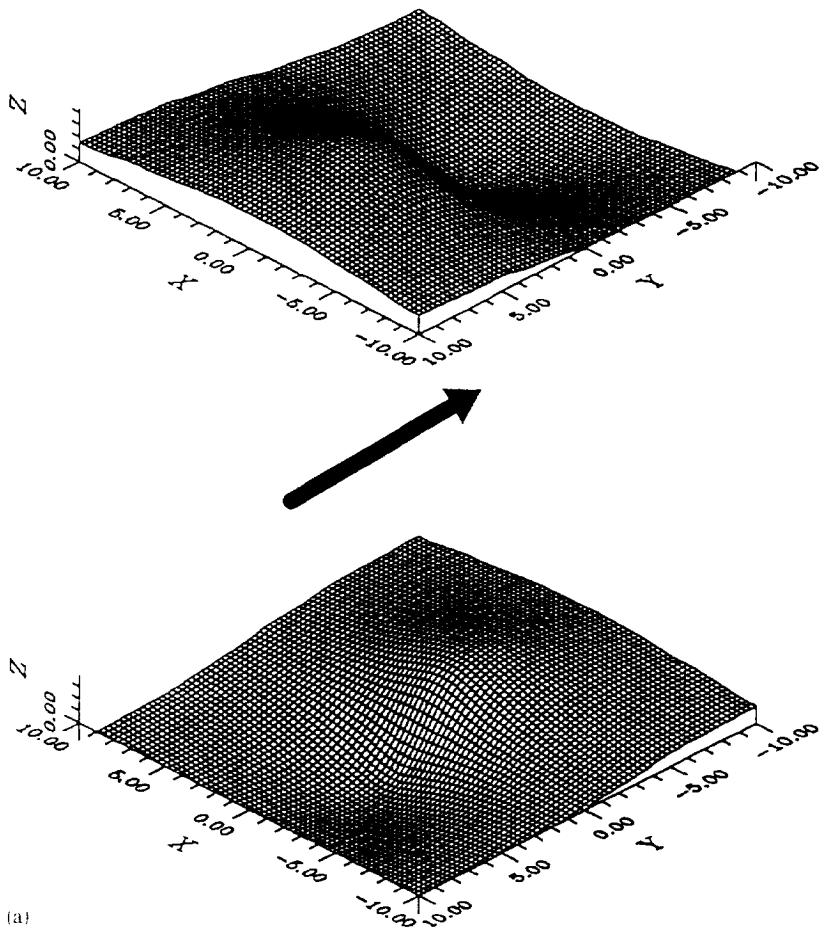

Fig. 9(a).

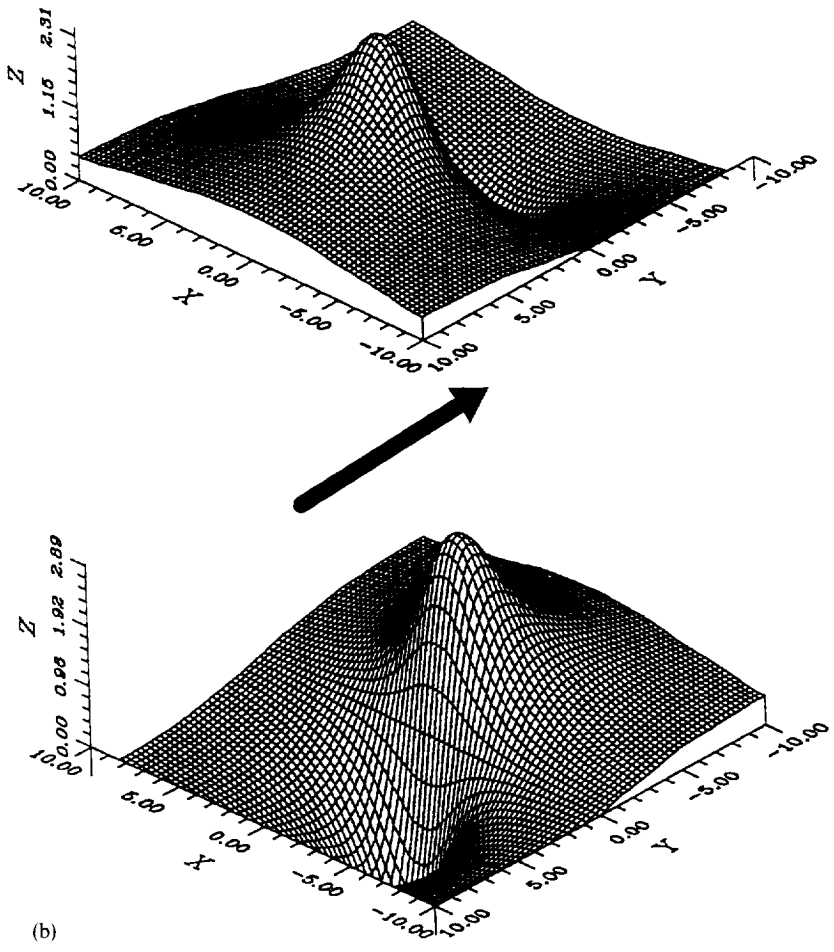

Fig. 9. Disturbances of the interface contours for the film boundaries for $z_1 = -1.5$, $z_2 = 2.0$, $K_d = 1.0$ and $E_d = 1.0$, $K_1 = 0.1$ and $E_1 = 0.1$, $K_2 = 0.1$ and $E_2 = 0.1$: viscosity ratios: (a) $\mu^f = 1.0$, $\mu^d = 1.0$ and (b) $\mu^f = 0.003$, $\mu^d = 1.0$.

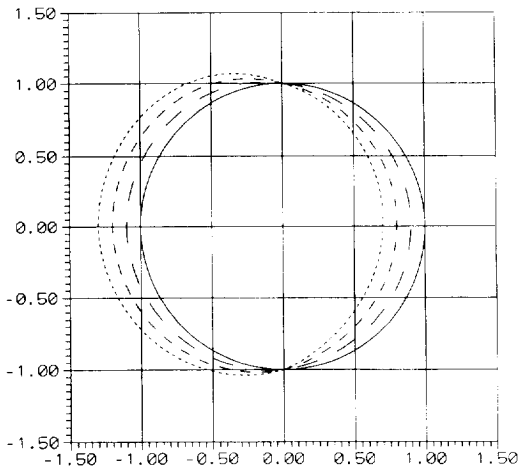

Fig. 10. Disturbances of the droplet interface for low viscous interfaces and for $z_1 = -1.2$ and $z_2 = 2.8$: (———) unperturbed surface; (— — —) capillary number 0.1; (- - -) capillary number 0.2 and (. . . .) capillary number 0.3.

same order of magnitude as the droplet and the surface viscosity, is considerably smaller for mobile surfaces than for rigid walls. However, if the film viscosity is very small compared to the droplet and the surface viscosity, the situation is very similar to the one calculated by Shapira and Haber and hence the drag coefficients are very much alike.

From Table 2 one can deduce that when the film viscosity is kept constant and larger than the droplet viscosity, there is almost no influence of the droplet viscosity numbers. Increasing the surface viscosity leads to higher drag coefficients which will eventually reach the values of Shapira and Haber for solid walls.

4. CONCLUSIONS

The presented method for the calculation of the fluid flow inside and outside an interfacial viscous droplet moving in a thin liquid film proved to be appropriate to investigate in detail the influence of various parameters relevant in such systems in detail.

It could be shown that the type and amount of surfactants, resulting in varying surface viscosities at the film surface as well as the droplet surface, does have a considerable influence on the flow pattern as well as on the drag coefficient of the moving drop. Besides, the calculations could shed some light on the mechanisms governing the behaviour of technically important systems, for example, emulsions of light and heavy oil in water. However, the resultant information on the behaviour of a single fluid particle in the film is of particular importance to coated films. The comparison with the calculations of Shapira and Haber (1988, 1990) revealed the strong influence of the surface properties on the drag exerted on the droplet.

Acknowledgements—We are indebted to Professor I. B. Ivanov for the most helpful discussions. Besides, we are grateful for the advice provided by Dr. H. Raszillier.

This work was supported financially by the "Volkswagen-Stiftung". The authors gratefully acknowledge this support of their collaborative research.

REFERENCES

Boussinesq, M. J., 1913, Sur l'éxistance d'une viscosité superficielle, dans la mince couche de transition separant un liquide d'une autre fluide contigue. *Ann. Chim. Phys.* **29**, 349–357.

Danov, K. D., Aust, R., Durst, F. and Lange, U., 1994, Influence of the surface viscosity on the drag and torque coefficients of a solid particle in a thin liquid layer. *Chem. Engng Sci.* **50**, 263–277.

Davis, R. H., 1993, Microhydrodynamics of particulate suspensions. *Adv. Colloid and Interface Sci.* **43**, 17–50.

Edwards, D. A., Brenner, H. and Wasan, D. T., 1991, *Interfacial Transport Processes and Rheology*. Butterworth-Heinemann, Boston.

Feng, S.-S., 1993, Determination of diffusion coefficient and rheological properties of surface layers from surface trough diffusion. *J. Colloid Interface Sci.* **160**, 449–458.

Hadamard, J. S., 1911, Mouvement permanent lent d'une sphere liquide et visqueuse dans un liquide visqueux. *Comp. Rend. Acad. Sci.* (Paris) **152**, 1735–1738.

Happel, J. and Brenner, H., 1965, *Low Reynolds Number Hydrodynamics with Special Applications to Particulate Media*. Prentice Hall, Englewood Cliffs, NJ.

Hetsroni, G., 1982, in *Handbook of Multiphase System* (Edited by G. Hetsroni). Hemisphere, Washington.

Hunter, R. J., 1987, *Foundation of Colloid Science*, Vol. I. Clarendon Press, Oxford.

Hunter, R. J., 1989, *Foundation of Colloid Science*, Vol. II. Clarendon Press, Oxford.

Lebedev, A. A., 1916, *Zhur. Russ. Fiz. Khim.* **48**.

Levich, V. G., 1962, *Physicochemical Hydrodynamics*. Prentice Hall, Englewood Cliffs, NJ.

Liron, N. and Barta, E., 1992, Motion of a rigid particle in Stokes flow: a new second-kind boundary-integral equation formulation. *J. Fluid Mech.* **238**, 579–598.

Mukhopadhyay, A., Sundararajan, T. and Biswas, G., 1993, An explicit transient algorithm for predicting incompressible viscous flows in arbitrary geometry. *Int. J. Numer. Meth. Fluids* **17**, 975–993.

Rybczynski, W., 1911, *Bull. Intern. Acad. Sci.* Cracovie (Ser. A), YO.

Scriven, L. E., 1960, Dynamics of a fluid interface. *Chem. Engng Sci.* **12**, 98–108.

Shapira, M. and Haber, S., 1988, Low Reynolds number motion of a droplet between two parallel flat plates. *Int. J. Multiphase Flow* **14**, 483–506.

Shapira, M. and Haber, S., 1990, Low Reynolds number motion of a droplet in shear flow including wall effects. *Int. J. Multiphase Flow* **16**, 305–321.

Silvey, A., 1916, The fall of mercury droplets in a viscous medium. *Phys. Rev.* **7**, 106–111.

Valentini, J. E., Thomas, W. R., Sevenhuysen, P., Jiang, T. S., Lee, O. H., Liu, Yi and Yen, S.-C., 1991, Role of dynamic surface tension in slide coating. *Ind. Engng Chem. Res.* **30**, 453–461.

Yang, S.-M. and Leal, L. G., 1990, Motion of a fluid drop near a deformable interface. *Int. J. Multiphase Flow* **16**, 597–616.